Inorganic Chemistry

pubs.acs.org/IC

Article

Nickel–Borolide Complexes and Their Complex Electronic Structure

Sam Yruegas, Hao Tang, Gayle Z. Bornovski, Xiaojun Su, Siyoung Sung, Michael B. Hall,* Michael Nippe,* and Caleb D. Martin*

Cite This: *Inorg. Chem.* 2021, 60, 16160–16167

Read Online

ACCESS | Metrics & More | Article Recommendations | Supporting Information

ABSTRACT: Borolides (BC_4^{2-}) can be considered as dianionic heterocyclic analogues of monoanionic cyclopentadienides. Although both are formally six-π-electron donors, we herein demonstrate that the electronic structure of their corresponding transition metal complexes differs significantly, leading to altered properties. Specifically, the 18-electron sandwich complex $Ni(iPr_2NBC_4Ph_2)_2$ (**1**) features an ~90° angle between the Ni–B–N planes and is best described as a combination of three limiting resonance structures with the major contribution stemming from a formally Ni^{2+} species bound to two monoanionic radical ($BC_4^{\bullet-}$) ligands. Compound **1** displays two sequential one-electron oxidation events over a small potential range of <0.2 V, which strikingly contrasts the large potential separations between redox partners in the family of metallocenes, and the potential reasons for this unusual observation are discussed.

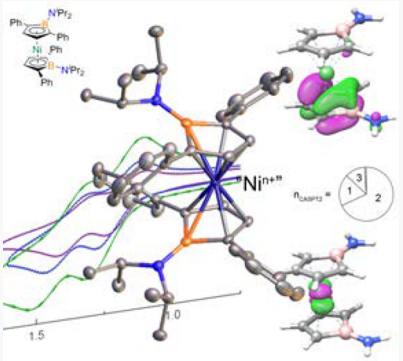

INTRODUCTION

The monoanionic cyclopentadienide ligand [Cp = $(C_5H_5)^-$] is ubiquitous to transition metal chemistry.[1] The η^5 binding mode allows access to a large variety of metallocenes (MCp_2)[2] as well as piano stool complexes ($MCpL_n$).[3] Transition metal (TM)-based metallocenes are stabilized by synergistic ligand-to-metal π-donating and metal-to-ligand δ-back-donating interactions between the six-π-electron donor Cp ligands and TM-based d orbitals, resulting in 18-, 19-, and 20-electron complexes for Fe^{2+}, Co^{2+}, and Ni^{2+}, respectively.[2g,h] Among the attractive properties of metallocenes, the reversible one-electron redox chemistry of the $[MCp_2]^{+/0}$ redox couple is frequently exploited. Thus, ferrocene (17/18 e^-) is one of the most popular internal reference materials for electrochemical studies in organic media, and cobaltocene (18/19 e^-) is a common powerful one-electron reductant.[1g] More recently, metallocene-based redox chemistry has also allowed the development of improved non-aqueous redox flow batteries (RFBs)[4] as well as electrolyte-free dye-sensitized solar cells.[5] The redox chemistry of the metallocenes extends well beyond the $[MCp_2]^{+/0}$ redox couple exemplified in electrochemical studies by Bard et al.,[6] in which an exotic 21-electron nickel species, $[NiCp_2]^-$, could be accessed.

The electrochemical potentials of the redox families of the metallocenes follow (for most cases) a direct correlation with ionization potentials of the transition metal ion as a consequence of mostly metal-centered redox events. The latter has been confirmed, in many examples, such as the isolation and characterization of $[FeCp^*_2]^{2+}$ [$Cp^* = (C_5Me_5)^-$] as an Fe^{4+} species[7] and the formulation of high-spin Fe^+ in $[Fe(Cp^{ttt})_2]^-$ [$Cp^{ttt} = (C_5H_2{}^tBu_3)^-$].[8] However, it is this relationship that results in very large potential separations between two electron redox partners (*vide infra*) and requires extreme potentials to access all members of a $[MCp_2]^{n+}$ redox series.

In contrast to the significant advances in the chemistry of cyclopentadienide complexes in the areas of catalysis,[1c] redox probes,[1g] and single-molecule magnets[1b] (among others) and a plethora of available ligand derivatives, their heteroatom analogues are much less developed, including boron-containing heterocycles. Boroles and borolides are unsaturated BC_4 and BC_4^{2-} ring systems that are anti-aromatic and aromatic, respectively, and can bind to metals in an η^5 fashion, analogous to the case for cyclopentadienide.[9] Upon coordination to metal ions, these unique ligands could formally be described as neutral four-π-electron donors, anionic five-π-electron systems, or dianionic six-π-electron ligands. This versatility renders their electronic structure complex and allows them to act as potential electron reservoirs, thereby generating a new class of redox-active ligands. Few studies have attempted to ascertain the redox activity or non-innocence of borolides. In this work, we synthesize a borolide and borole as precursors to ultimately access the sandwich complex $Ni(iPr_2NBC_4Ph_2)_2$ [**1** (Figure 1)] and a half-sandwich variant as a model series to probe the electronic structure. Nickel was selected as possible resonance structures can be drawn for **1** featuring formal Ni^0,

Received: June 17, 2021
Published: October 12, 2021

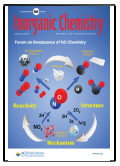

https://doi.org/10.1021/acs.inorgchem.1c01845
Inorg. Chem. 2021, 60, 16160–16167

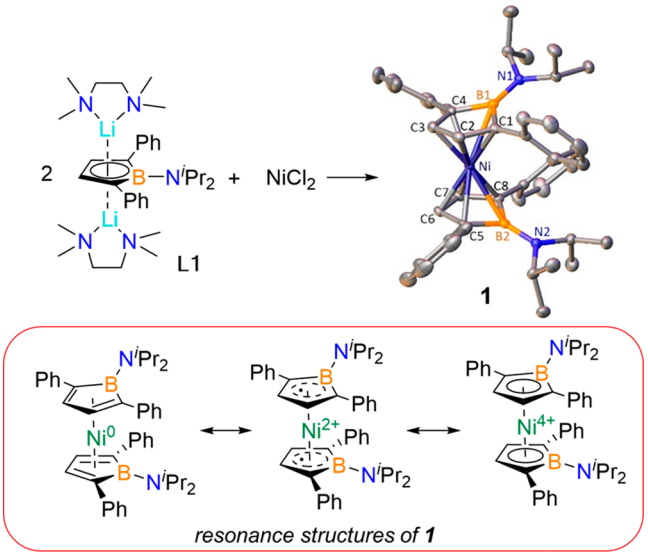

Figure 1. Synthesis of **1** from borolide **L1** and molecular structure of **1** (top). Resonance structures of **1** (bottom). Hydrogen atoms and co-crystallized solvent molecules have been omitted for the sake of clarity. Thermal ellipsoids depicted at the 50% probability level.

Ni^{2+}, or Ni^{4+} species (Figure 1, bottom). Within the realm of high-oxidation state nickel chemistry,[10] it has been documented that there is ambiguity in assigning oxidation states. Although a limited number of the latter high-oxidation state compounds have been reported,[11] the decamethylnickelocene dication, described as nickel(IV), has been known since the early 1980s.[12] In recent years, significant interest has been paid to discerning whether elusive Ni^{4+} species are viable in catalytic cross-coupling.[13] The homoleptic and heteroleptic Ni–borolide species were evaluated using a combination of spectroscopic, electrochemical, and computational methods to understand the bonding in metal–borolide complexes.

RESULTS AND DISCUSSION

Deprotonation of 1-diisopropylamino-2,5-diphenyl-3-borolene[14] with LDA in the presence of TMEDA furnishes the dilithioborolide in 65% yield {Figure 2, $[Li(TMEDA)]_2[2,5\text{-}iPr_2NBC_4Ph_2]$, **L1**}. The ^{11}B nuclear magnetic resonance (NMR) resonance observed for **L1** (26.9 ppm) is consistent

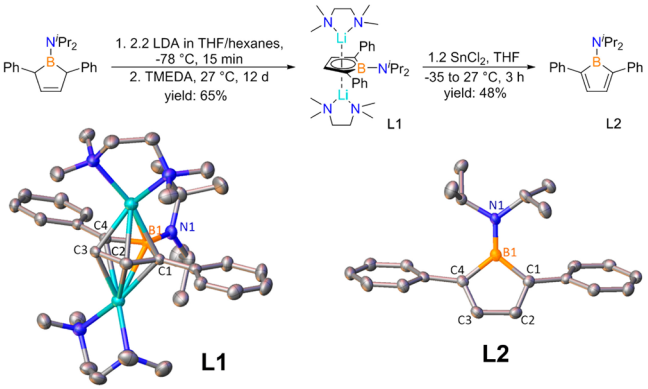

Figure 2. Synthesis of borolide **L1** and borole **L2** (top). Molecular structures of **L1** (left) and **L2** (right) (bottom). Hydrogen atoms and co-crystallized solvent molecules have been omitted for the sake of clarity. Thermal ellipsoids depicted at the 50% probability level.

with the reported dilithium borolide salts.[15] Single-crystal X-ray diffraction studies reveal an η^5 mode of coordination of the ligand to the two lithium ions above and below the plane (Figure 2). Oxidation of **L1** with tin(II) chloride results in the formation of the neutral 1-diisopropylamino-2,5-diphenylborole (**L2**) in 48% yield after workup. The ^{11}B NMR signal of **L2** is shifted downfield to 39.2 ppm upon oxidation. It is unusual that this borole species is monomeric, given that boroles devoid of bulky groups are prone to [4+2] Diels–Alder dimerization.[16] We next targeted the isolation of Ni–borolide complexes.

Borolide transition metal complexes have previously been accessed via the functionalization of coordinated ligands,[17] dehydrogenation of 3-borolenes,[18] complexation of cationic metal precursors with borolide dianions,[15a,16c,19] or coordination of neutral boroles to low-oxidation state metal ions.[15d,20] Metalation of **L1** with $NiCl_2$ using a 1:1 stoichiometry generated Ni(0) and LiCl as well as a species with a ^{11}B NMR spectroscopic resonance at 28.0 ppm. The boron-containing species was purified by column chromatography and isolated as a deep red solid in 16% yield that was identified as the desired sandwich complex $Ni(iPr_2NBC_4Ph_2)_2$ [**1** (Figure 3)]. The formation of Ni(0) implies the possibility for

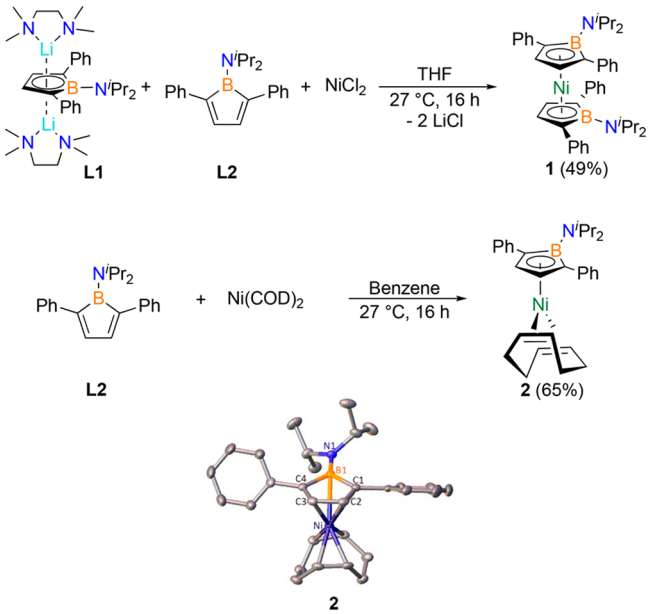

Figure 3. Synthesis of **1** and **2** (top). Molecular structure of **2** (bottom). Hydrogen atoms and co-crystallized solvent molecules have been omitted for the sake of clarity. Thermal ellipsoids depicted at the 50% probability level.

reduction of Ni^{2+} by **L1** with concomitant formation of a monoanionic borole.[21] The latter can also be viewed as comproportionation products of dianionic borolides and neutral boroles. The isolation of a monoanionic borole from either comproportionation of **L1** and **L2** or the one-electron reduction of borole **L2** was unsuccessful.[22] However, consistent with the considerations mentioned above, the yield for the formation of **1** can be significantly improved (49%) if 1 equiv of neutral borole **L2** is added to a stoichiometric mixture of **L1** and $NiCl_2$.[23]

Access to the heteroleptic complex Ni(COD)-$(iPr_2NBC_4Ph_2)$ (**2**) is achieved by the stoichiometric reaction of neutral borole **L2** and $Ni(COD)_2$ in benzene (Figure 3).

https://doi.org/10.1021/acs.inorgchem.1c01845
Inorg. Chem. 2021, 60, 16160–16167

The formation of **2** under our conditions is comparable to the preparation of group 10 TM(COD)(C_4H_4BR) (TM = Ni, Pd, or Pt) complexes via the reactions of $TM(COD)_2$ with borole ammonia adducts, such as $C_4H_4BR{\cdot}NH_3$ (R = CH_3 or Ph), as reported by Herberich et al.[17a] The observed ^{11}B NMR resonance of **2** (26.0 ppm) is shifted significantly upfield compared to that of free **L2** and is consistent with other (η^5-borolide)Ni(1,5-cyclooctadiene) complexes.[17b,20a] Complex **2** was isolated as a red solid in 65% yield after workup, and its molecular structure established via single-crystal X-ray diffraction (Figure 3).

The solid state structures of neutral borole **L2**, dilithio salt **L1**, and nickel complexes **1** and **2** (Tables S1 and S2) display significant differences in the molecular geometries of the heterocycle. While the BC_4 heterocycle of aromatic **L1** is planar and that of anti-aromatic **L2** deviates only slightly from planarity (maximum deviation from planarity of 0.002 Å for **L1** and 0.078 Å for **L2**), both nickel complexes show considerable contortion, with sandwich complex **1** being the most puckered (**1**, average deviation from planarity of both rings of 0.262 Å; **2**, 0.133 Å). The phenyl groups in the structures of **L2**, **1**, and **2** are twisted with respect to the central BC_4 ring, while **L1** features essentially co-planarity (interplanar angles of 6.16° and 1.80°). The diene backbone of **L2** contains localized bonds [C(1)−C(2), 1.345(2) Å; C(2)−C(3), 1.470(2) Å; C(3)−C(4), 1.347(2) Å] consistent with the four-π-electron anti-aromatic electronic configuration, while all intraring bond lengths in **L1**, **1**, and **2** are consistent with π-electron delocalization [range of 1.393(2)−1.447(2) Å]. The B−N bond is the shortest in anti-aromatic **L2** [1.390(2) Å] but only marginally longer in the nickel complexes [**1**, 1.414(3) Å; **2**, 1.429(2) Å], consistent with a π-donor interaction from the nitrogen lone pair to the boron center [cf. $HB(NH_2)_2$, 1.418 Å].[24] The aromatic dianionic species **L1** has a much longer B−N bond [1.513(2) Å], which is attributed to the aromaticity of the ring and the co-planar phenyl groups. In sandwich complex **1**, the η^5-borole ligands have a 72° rotary angle around the borole−Ni−borole central axis. The nickel−boron bonds in **1** and **2** [for **1**, B(1)−Ni = 2.397(3) Å and B(2)−Ni = 2.424(2) Å; for **2**, B(1)−Ni = 2.388(2) Å] are longer than those to the carbon atoms [**1**, Ni−C range of 2.000(3)−2.147(2) Å; **2**, 2.040(2)−2.196(2) Å].

Although some examples of $Ni(BC_4)_2$-type species have been reported,[16c,17b,18d,19b] very limited analytical data exist and only one compound has been crystallographically characterized. The Ni−B and Ni−C bond distances in **1** are marginally longer than those in a complex featuring two Ni(η^5-BC_4)$_2$ units linked by 1,3-dipropoxides on boron [Ni−B range of 2.200(1)−2.234(1) Å; Ni−C range of 1.956(1)−2.122(1) Å]. In contrast to **1** in which the BC_4 rings are puckered, the rings within the dinickel complex are planar, perhaps attributable to the change from amino to alkoxy substitution on boron (maximum deviations from planarity of 0.070 and 0.097 Å).[19b] Half-sandwich complex **2** may be best compared to a 9-borafluorene complex recently reported by Harman, which features a 0.251 Å shorter Ni−B bond and longer Ni−C bonds [range of 2.212(2)−2.238(2) Å], likely as a consequence of the rigidity imposed by the pendent phosphine on the 9-borafluorene-phosphine ligand.[25]

The redox properties of **1** and **2** (1 mM) were investigated by means of cyclic voltammetry in CH_2Cl_2 (0.1 M NBu_4PF_6) under an Ar atmosphere. The cyclic voltammogram (CV) of **2** (Figure S28) displays one oxidation event centered at −0.34 V versus $Fc^{0/+}$ closely followed by a second oxidation event at −0.18 V versus $Fc^{0/+}$ that features a significantly smaller current density. We tentatively ascribe these observations to the limited stability of *in situ*-formed $\mathbf{2}^+$ that rearranges to an unknown species that is oxidized at −0.18 V. In agreement with this formulation, the intensity of the second oxidation decreases and the reversibility of the initial oxidation feature improves with increasing scan rates. The CV of **1** (Figure 4) shows two quasi-reversible oxidation waves at 1.14 and 1.32 V versus $[CoCp_2]^{0/+}$ (−0.19 and −0.01 V, respectively, vs $Fc^{0/+}$) at a scan rate of 100 mV s^{-1}.

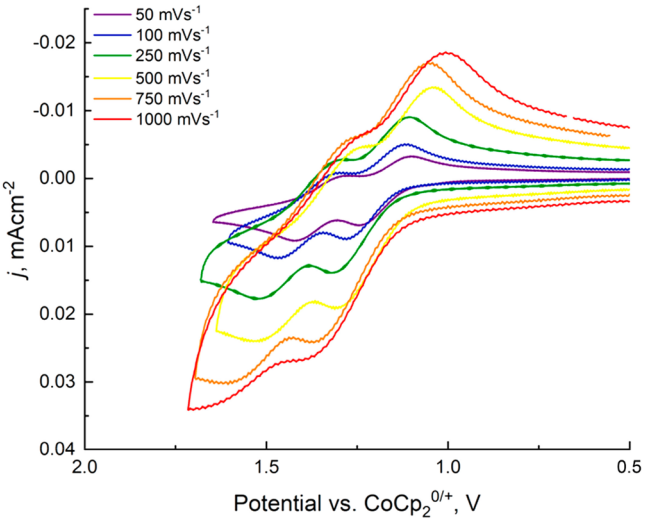

Figure 4. Cyclic voltammograms of **1** (1 mM) in CH_2Cl_2 (0.1 M NBu_4PF_6) at varying scan rates as indicated in the inset.

These observations are remarkable for two reasons. (i) The presence of two oxidations is in stark contrast to the irreversible oxidation events reported for $Ni(C_4H_4BR)_2$ sandwich complexes[19b] and may indicate the importance of phenyl substituents for the stabilization of the mono- and dicationic species. (ii) The fact that both oxidations occur over a very small potential range of ∼0.2 V (even in the fairly nonpolar solvent CH_2Cl_2) contrasts the large potential separations between redox couples observed for metallocenes (Figure 5). The first oxidation is assigned to the $\mathbf{1}/\mathbf{1}^+$ redox

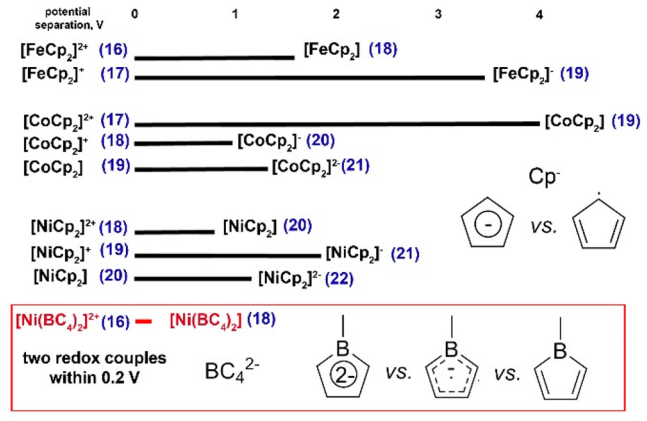

Figure 5. Potential separations between two-electron varying $[MCp_2]^{n+}$ species[6] and those observed in CVs of new nickel sandwich complex **1**.

https://doi.org/10.1021/acs.inorgchem.1c01845
Inorg. Chem. 2021, 60, 16160−16167

couple that remains reversible over the employed scan rates albeit features >59 mV E_a to E_p separations. The latter is likely due to significant reorganization of the solvation shell upon electron transfer. Initial attempts to isolate $\mathbf{1}^+$ have not been successful, but we are able to computationally predict the geometry of $\mathbf{1}^+$ and show that $\mathbf{1}^+$ is not expected to feature a Ni^{3+} ion but rather a Ni^{2+} ion with the single anionic charge delocalized over the whole molecule (vide infra). Assuming the absence of unknown side reactions of $\mathbf{1}^+$, including potential linkage isomerization,[26] we tentatively assign the second oxidation to the $\mathbf{1}^+/\mathbf{1}^{2+}$ redox couple. Compound $\mathbf{1}^{2+}$ is expected to be very reactive and may not be isolatable under standard conditions. This may contribute to the somewhat attenuated reversibility of this redox couple in the CV.

Given the preceding discussion and the ambiguous nature of the electronic structures of nickel complexes **1** and **2**, density functional theory (DFT) calculations were performed using Gaussian 09[27] (see the Supporting Information for computational details). Benchmarking of DFT functionals was carried out by comparing the optimized gas phase geometries of **L1**, **L2**, **1**, and **2** (Tables S3−S6) to those experimentally observed and identified TPSSh as the appropriate functional for this study. The singlet state is calculated to be lower in free energy than the triplet (quintet) state by 22.6 (50.7) and 20.7 (80.2) kcal/mol for **1** and **2**, respectively, in agreement with the experimentally observed diamagnetic nature of both compounds. Consistent with the experimental result, the geometric parameters of the heterocycles in **1** are similar to those calculated for a monoanionic radical species $[iPr_2NBC_4Ph_2]^-$ (Table S7) and are intermediate between those obtained for neutral **L2**, and those for **L1**, and a hypothetical uncoordinated borolide dianion (Table S8), which suggests monoanionic heterocycles in **1** and a Ni oxidation state of closer to +2 rather than 0 or +4. Likewise, DFT calculations predict that the geometric parameters of the heterocycle in **2** are also consistent with a monoanionic species $[iPr_2NBC_4Ph_2]^-$ (Table S7), and a Ni^+ center. The key geometric distinction is the difference in length between the C−C bond opposite of B and those adjacent, which computationally are 0.12 Å for neutral **L2**, 0.01 Å for the monoanion, −0.06 Å average for **L1** and the uncoordinated dianion, 0.02 Å for **1**, and 0.04 Å for **2**. Thus, the comparison of C−C bond lengths across this series clearly points toward the monoanionic radical form of the ligand $[iPr_2NBC_4Ph_2]^-$ in Ni complexes **1** and **2**.

Inspection of the DFT-calculated frontier orbitals (Figures S30 and S31) reveals that there is strong metal−ligand mixing in the frontier orbitals of **1′** and **2′** (truncated models of **1** and **2**, respectively, in which ^{i}Pr and Ph are replaced with H), with significant ligand character in the HOMO and HOMO−1. The MOs appear to be so highly delocalized between Ni and the ligands that assigning these electrons to the Ni to produce a formal Ni(0) oxidation state or assigning them to the ligands to produce a formal Ni(IV) oxidation state would be equally possible but perhaps equally incorrect. To explore the nature of this delocalization, we performed higher-level, multireference CASSCF(4,4) and CASPT2(4,4) single-point calculations on the truncated model (**1′**, ^{i}Pr and Ph replaced with H) at the def2-TZVP (all of the atoms) level similar to previous work.[28,29] The CASSCF singlet state of **1′** shows eight configurations ($\mathbf{\Psi}_1$−$\mathbf{\Psi}_8$) (Figure 6). The leading configuration ($\mathbf{\Psi}_1$) has two highly delocalized Ni-L′ π-bonding orbitals (ψ_1 = Ni-d_{xz} + L′-π, and ψ_2 = Ni-d_{yz} + L′-π) doubly occupied. The next two most important configurations ($\mathbf{\Psi}_2$ and $\mathbf{\Psi}_3$) represent paired two-e$^-$ excitations from these bonding MOs to their antibonding MOs (ψ_4 and ψ_3), respectively (Figure 6). The other configurations ($\mathbf{\Psi}_4$−$\mathbf{\Psi}_8$) with somewhat smaller coefficients represent split two-e$^-$ excitations from the bonding MOs to the antibonding MOs, except for $\mathbf{\Psi}_6$, which is the four-e$^-$ excitation. This wave function results in electron occupancy numbers of ψ_1 (1.81) and ψ_2 (1.80) for the bonding MOs and ψ_3 (0.20) and ψ_4 (0.19) for the antibonding MOs. This delocalized description is consistent with the DFT results, but such high occupation numbers for the antibonding MOs suggest that the delocalized nature of these MOs is so strong that a valence bond (VB) representation would yield a more consistent and correct description of the oxidation state.

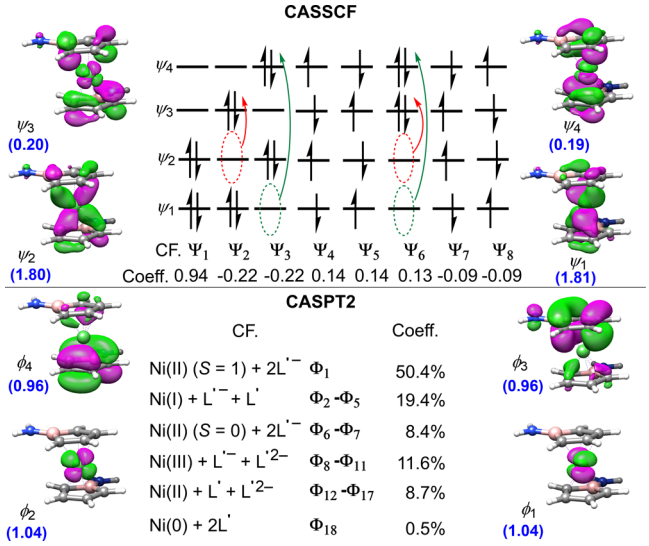

Figure 6. (a) CASSCF and (b) CASPT2 of the singlet state for **1′**. (a) Main electronic configurations ($\mathbf{\Psi}_i$), key natural orbitals (ψ_i), and electron occupancy numbers (blue) for CASSCF(4,4). (b) Main electronic configurations ($\mathbf{\Phi}_i$), localized orbitals (ϕ_i), and electron occupancy numbers (blue) for CASPT2(4,4). All of the configurations for CASPT2 are listed in Table S11.

Discussion of the formal Ni oxidation state may be informed by considering the localized VB representation of this wave function that is generated for the CASPT2 calculations (Figure 6, bottom). These VB orbitals show that the principal configuration $\mathbf{\Phi}_1$ with a coefficient of 0.71 is a Ni^{2+} (S = 1) center bound to two borolide radical anions [two singly occupied Ni d orbitals, ϕ_1 (Ni-d_{xz}) and ϕ_2 (Ni-d_{yz}) of the same spin with strong antiferromagnetic coupling to two singly occupied **L′** orbitals, ϕ_3 (L′-π) and ϕ_4 (L′-π)]. The contributions of the other configurations are shown in Figure 6 and Table S11. Overall, the VB-localized representation can be interpreted as involving the following oxidation states: 68% Ni^{2+} + 19% Ni^+ + 12% Ni^{3+} + 1% Ni^0. These percentages are consistent with the structures corresponding to monoanionic ligands. The CASPT2 calculation produces electron occupancy numbers of 1.04, 1.04, 0.96, and 0.96 for ϕ_1 (Ni-d_{xz}), ϕ_2 (Ni-d_{yz}), ϕ_3 (L′-π), and ϕ_4 (L′-π), respectively, reflecting the conclusion that the singlet state of **1** is best described as a Ni^{2+} center with strong antiferromagnetic (VB) coupling between two singly occupied Ni d_{xz} and d_{yz} orbitals and two singly occupied L′-π-orbitals. Note that CASSCF calculations with larger active orbital spaces did not provide a qualitatively different solution.

https://doi.org/10.1021/acs.inorgchem.1c01845
Inorg. Chem. 2021, 60, 16160−16167

The formalism of the oxidation state in metal complexes with highly covalent interactions, inverted ligand fields, or delocalized electronic structures frequently attracts vigorous debate. In addition to the ab initio calculations discussed above, which clearly point toward the multiconfigurational nature of the ground state electronic structure of **1** (and a main component equivalent to a Ni^{2+} description), it can also be informative to consider changes in bond dissociation energies within a series of NiL_2 complexes, ranging from "clear-cut" Ni^{2+} to "clear-cut" Ni^0 complexes.

As shown in Figure 7, the bond dissociation energy for $Ni(COD)_2$, an unequivocal bis(diene) complex of Ni^0, is

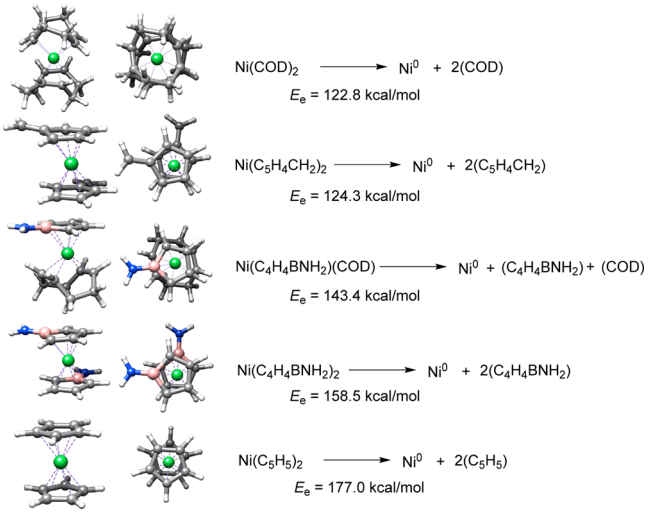

Figure 7. Bond dissociation energies of various Ni complexes show a clear trend. The left to right structures are the side and top views, respectively.

calculated to be 123 kcal/mol, which is much smaller than that of $NiCp_2$ (177 kcal/mol), which would be considered to be a prototypical organometallic Ni^{2+} complex. The dissociation energy of model complex **1′** is ∼36 kcal/mol larger than that of $Ni(COD)_2$ and only ∼18 kcal/mol smaller than that of $NiCp_2$. Similarly, model complex **2′** has an intermediate bond energy consistent with a strong Ni^+ character and one neutral diene ligand and one anionic borolide ligand making a covalent bond to Ni. Interestingly, the $Ni(fulvene)_2$, which is isoelectronic to complex **1′**, is also much more weakly bound and only ∼2 kcal/mol more strongly bound than $Ni(COD)_2$. Finally, all ligand−Ni bond lengths for model complex **1′** are shorter than those for the fulvene complex, and even the B−Ni bond is shorter than the corresponding Ni−C bond (see Figure S36).

One might wonder how boroles become such good acceptors in these Ni complexes when the reduction of boroles to form borolide anions otherwise requires fairly strong reducing agents. Figure 8 illustrates how the nearly 90° arrangement of one N−B−Ni plane with respect to the other produces synergism between one ring's acceptor orbital (upper) and the other ring's donor orbital (lower). Doubly occupied 3d orbitals on a Ni^0 act as bridges by shifting substantial electron density from these 3d orbitals into the acceptor orbitals to accommodate electrons from the donor orbitals. This synergism, which takes place in two orthogonal planes, contributes to the unexpectedly strong acceptor characteristics of the ligands and at the same time could explain the small potential separation between the two redox

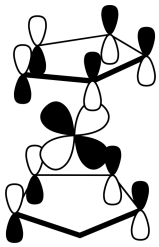

Figure 8. Depiction of the metal−ligand bonding orbital rationalizing the orientations of the borolide rings.

events observed in CVs of **1**. Because of the orthogonal nature of this synergism, even the simple truncated model complex **1′** has two rotational barriers (both ∼10 kcal/mol above the minimium energy structure) where the two N−B−Ni planes are at 0° and 180° (Figure S35). Interestingly, for calculated monocation $\mathbf{1}^+$ (doublet ground state) (Figure S33), two equal-energy, rotational minima at ∼90° and 180° are found, which display quite different spin distributions. Specifically, the 90° isomer features a spin population distributed equally among the Ni and both ligands, while the spin population of the 180° isomer appears to be split between the two ligands with no involvement of Ni (Table S13). On the contrary, calculated dicationic $\mathbf{1}^{2+}$ (Figure S34) is calculated to have a singlet ground state with rotational minima at ∼0° and 180° and a barrier at ∼90° consistent with the second electron also being removed from orbitals with mainly ligand character.

CONCLUSIONS

In summary, we synthesized and characterized a dilithium borolide, neutral borole, and their nickel sandwich and half-sandwich complexes. All feature a diisopropylamino group on boron and phenyl groups on the adjacent carbon centers, permitting a thorough structural comparison of the molecules. DFT, CASSCF, and CASPT2 calculations indicate that sandwich complex **1** is best described as a Ni^{2+} triplet ion spin-coupled (bonded) to two monoanionic radical ($BC_4^{\bullet-}$) species, whereas **2** is defined as a Ni^+ center bonded to a monoanionic radical ligand. Compound **1** displays two quasi-reversible one-electron oxidation events within a remarkably miniscule potential window of <200 mV. This stands in stark contrast to the large potential separations observed for the ubiquitous first-row metallocenes in which their frontier orbitals reside predominantly on the metal.

ASSOCIATED CONTENT

Supporting Information

The Supporting Information is available free of charge at https://pubs.acs.org/doi/10.1021/acs.inorgchem.1c01845.

^1H and ^{11}B NMR and UV−vis spectra, cyclic voltammetry data, crystallographic data, computational details, and DFT coordinates (PDF)

Accession Codes

CCDC 2053824−2053828 contain the supplementary crystallographic data for this paper. These data can be obtained free of charge via www.ccdc.cam.ac.uk/data_request/cif, or by emailing data_request@ccdc.cam.ac.uk, or by contacting The Cambridge Crystallographic Data Centre, 12 Union Road, Cambridge CB2 1EZ, UK; fax: +44 1223 336033.

https://doi.org/10.1021/acs.inorgchem.1c01845
Inorg. Chem. 2021, 60, 16160−16167

AUTHOR INFORMATION

Corresponding Authors

Michael B. Hall − *Department of Chemistry, Texas A&M University, College Station, Texas 77843, United States*; Email: hall@science.tamu.edu

Michael Nippe − *Department of Chemistry, Texas A&M University, College Station, Texas 77843, United States*; orcid.org/0000-0003-1091-4677; Email: nippe@tamu.edu

Caleb D. Martin − *Department of Chemistry and Biochemistry, Baylor University, Waco, Texas 76798, United States*; orcid.org/0000-0001-9681-0160; Email: caleb_d_martin@baylor.edu

Authors

Sam Yruegas − *Department of Chemistry and Biochemistry, Baylor University, Waco, Texas 76798, United States*; orcid.org/0000-0002-8936-6847

Hao Tang − *Department of Chemistry, Texas A&M University, College Station, Texas 77843, United States*

Gayle Z. Bornovski − *Department of Chemistry, Texas A&M University, College Station, Texas 77843, United States*

Xiaojun Su − *Department of Chemistry and Biochemistry, Baylor University, Waco, Texas 76798, United States*

Siyoung Sung − *Department of Chemistry, Texas A&M University, College Station, Texas 77843, United States*

Complete contact information is available at: https://pubs.acs.org/10.1021/acs.inorgchem.1c01845

Notes

The authors declare no competing financial interest.

ACKNOWLEDGMENTS

C.D.M., M.N., and M.B.H. acknowledge support by The Welch Foundation (Grants AA-1846, A-1880, and A-0648, respectively). C.D.M. and M.B.H. thank the National Science Foundation (Grants 1753025 and CHE-1664866, respectively). Computer time was provided by the TAMU High-Performance Research Computing Facility, and software was provided by the Laboratory for Molecular Simulation.

REFERENCES

(1) (a) Chirik, P. J. Group 4 Transition Metal Sandwich Complexes: Still Fresh after Almost 60 Years. *Organometallics* **2010**, *29*, 1500−1517. (b) Day, B. M.; Guo, F. S.; Layfield, R. A. Cyclopentadienyl Ligands in Lanthanide Single-Molecule Magnets: One Ring To Rule Them All? *Acc. Chem. Res.* **2018**, *51*, 1880−1889. (c) Alt, H. G.; Licht, E. H.; Licht, A. I.; Schneider, K. J. Metallacyclic metallocene complexes as catalysts for olefin polymerization. *Coord. Chem. Rev.* **2006**, *250*, 2−17. (d) Choi, J.; Tang, L. H.; Norton, J. R. Kinetics of hydrogen atom transfer from (η^5-C_5H_5)Cr(CO)$_3$H to various olefins: Influence of olefin structure. *J. Am. Chem. Soc.* **2007**, *129*, 234−240. (e) Evans, W. J. Tutorial on the Role of Cyclopentadienyl Ligands in the Discovery of Molecular Complexes of the Rare-Earth and Actinide Metals in New Oxidation States. *Organometallics* **2016**, *35*, 3088−3100. (f) Wang, H. G.; Glorius, F. Lending Handedness to the Cyclopentadienyl Ligand. *Science* **2012**, *338*, 479−480. (g) Connelly, N. G.; Geiger, W. E. Chemical redox agents for organometallic chemistry. *Chem. Rev.* **1996**, *96*, 877−910.

(2) (a) Kealy, T. J.; Pauson, P. L. A New Type of Organo-Iron Compound. *Nature* **1951**, *168*, 1039−1040. (b) Miller, S. A.; Tebboth, J. A.; Tremaine, J. F. Dicyclopentadienyliron. *J. Chem. Soc.* **1952**, 632−635. (c) Wilkinson, G. The Preparation and Some Properties of the Cobalticinium Salts. *J. Am. Chem. Soc.* **1952**, *74*, 6148−6149. (d) Cotton, F. A.; Whipple, R. O.; Wilkinson, G. Bis-Cyclopentadienyl Compounds of Rhodium(III) and Iridium(III). *J. Am. Chem. Soc.* **1953**, *75*, 3586−3587. (e) Fischer, E. O.; Hafner, W. Di-Cyclopentadienyl-Chrom. *Z. Naturforsch., B: J. Chem. Sci.* **1953**, *8*, 444−445. (f) Wilkinson, G.; Birmingham, J. M. Bis-Cyclopentadienyl Compounds of Ti, Zr, V, Nb and Ta. *J. Am. Chem. Soc.* **1954**, *76*, 4281−4284. (g) Wilkinson, G.; Pauson, P. L.; Cotton, F. A. Bis-Cyclopentadienyl Compounds of Nickel and Cobalt. *J. Am. Chem. Soc.* **1954**, *76*, 1970−1974. (h) Fischer, E. O.; Pfab, W. Cyclopentadien-Metallkomplexe, Ein Neuer Typ Metallorganischer Verbindungen. *Z. Naturforsch., B: J. Chem. Sci.* **1952**, *7*, 377−379. (i) Werner, H. At Least 60 Years of Ferrocene: The Discovery and Rediscovery of the Sandwich Complexes. *Angew. Chem., Int. Ed.* **2012**, *51*, 6052−6058.

(3) (a) King, R. B.; Stone, F. G. A. Cyclopentadienyl Metal Carbonyls and Some Derivatives. *Inorg. Synth.* **1963**, *7*, 99−115. (b) Gress, M. E.; Jacobson, R. A. Crystal and Molecular Structure of π-$C_5H_5Fe(CO)_3PF_6$, a Cationic Iron Carbonyl Complex. *Inorg. Chem.* **1973**, *12*, 1746−1749. (c) Gill, T. P.; Mann, K. R. Photochemical Properties of the Cyclopentadienyl(η6-Benzene)Ruthenium(II) Cation. The Synthesis and Reactions of a Synthetically Useful Intermediate: the Cyclopentadienyltris(Acetonitrile)Ruthenium(II) Cation. *Organometallics* **1982**, *1*, 485−488. (d) Kubacek, P.; Hoffmann, R.; Havlas, Z. Piano-Stool Complexes of the CpML$_4$ Type. *Organometallics* **1982**, *1*, 180−188. (e) Gambarotta, S.; Chiesivilla, A.; Guastini, C. Synthesis, Reactivity, and Crystal Structure of CpV(CO)$_3$tht (tht = Tetrahydrothiophene). A Mild-Condition Synthetic Pathway to Substitution Derivatives of CpV(CO)$_4$ and Preparation and X-Ray Characterization of Cis-CpV(CO)$_2$bpy (bpy = 2,2′-Bipyridine). *Inorg. Chem.* **1988**, *27*, 99−102.

(4) (a) Ding, Y.; Zhao, Y.; Li, Y. T.; Goodenough, J. B.; Yu, G. H. A high-performance all-metallocene-based, non-aqueous redox flow battery. *Energy Environ. Sci.* **2017**, *10*, 491−497. (b) Milton, M.; Cheng, Q.; Yang, Y.; Nuckolls, C.; Hernández Sánchez, R.; Sisto, T. J. Molecular Materials for Nonaqueous Flow Batteries with a High Coulombic Efficiency and Stable Cycling. *Nano Lett.* **2017**, *17*, 7859−7863.

(5) Ghosh, A.; Mishra, S.; Giri, S.; Mobin, S. M.; Bera, A.; Chatterjee, S. Electrolyte-Free Dye-Sensitized Solar Cell with High Open Circuit Voltage Using a Bifunctional Ferrocene-Based Cyanovinyl Molecule as Dye and Redox Couple. *Organometallics* **2018**, *37*, 1999−2002.

(6) Bard, A. J.; Garcia, E.; Kukharenko, S.; Strelets, V. V. Electrochemistry of Metallocenes at Very Negative and Very Positive Potentials - Electrogeneration of 17-Electron Cp_2Co^{2+}, Cp_2Co^{2-}, and Cp_2Ni^{2-} Species. *Inorg. Chem.* **1993**, *32*, 3528−3531.

(7) Malischewski, M.; Adelhardt, M.; Sutter, J.; Meyer, K.; Seppelt, K. Isolation and structural and electronic characterization of salts of the decamethylferrocene dication. *Science* **2016**, *353*, 678−682.

(8) Goodwin, C. A. P.; Giansiracusa, M. J.; Greer, S. M.; Nicholas, H. M.; Evans, P.; Vonci, M.; Hill, S.; Chilton, N. F.; Mills, D. P. Isolation and electronic structures of derivatized manganocene, ferrocene and cobaltocene anions. *Nat. Chem.* **2021**, *13*, 243−248.

(9) Sadimenko, A. P. Organometallic Compounds of Pyrrole, Indole, Carbazole, Phospholes, Siloles, and Boroles. *Adv. Heterocycl. Chem.* **2001**, *79*, 115−157.

(10) Mitra, R.; Pörschke, K. R. Organonickel(IV) Chemistry: A New Catalyst? *Angew. Chem., Int. Ed.* **2015**, *54*, 7488−7490.

(11) (a) Bickelhaupt, A.; Lemke, M.; Sun, H.; Brand, A.; Jung, T.; Röhr, C.; Flörke, U.; Haupt, H.-J.; Klein, H.-F. Trimethylphosphine Complexes of Diorganonickel(IV) Moieties. *Organometallics* **1997**, *16*, 668−676. (b) Shimada, S.; Rao, M. L. N.; Tanaka, M. Reaction of 1,2-Disilylbenzene with Bis[1,2-bis(dimethylphosphino)ethane]-nickel(0). Isolation and Characterization of the First Silylnickel(IV) Complex. *Organometallics* **1999**, *18*, 291−293. Linden, A.; Dimitrov, V. A Pseudotetrahedral, High-Oxidation-State Organonickel Compound: Synthesis and Structure of Bromotris(1-norbornyl)nickel(IV). *Angew. Chem., Int. Ed.* **2003**, *42*, 2631−2633. (c) Carnes, M.; Buccella, D.; Chen, J. Y.-C.; Ramirez, A. P.; Turro, N. J.; Nuckolls, C.; Steigerwald, M. A Stable Tetraalkyl Complex of Nickel(IV). *Angew.*

Chem., Int. Ed. **2009**, *48*, 290−294. (d) Espinosa Martinez, G.; Ocampo, C.; Park, Y. J.; Fout, A. R. Accessing Pincer Bis(carbene) Ni(IV) Complexes from Ni(II) via Halogen and Halogen Surrogates. *J. Am. Chem. Soc.* **2016**, *138*, 4290−4293. (e) Kouno, M.; Yoshinari, N.; Kuwamura, N.; Yamagami, K.; Sekiyama, A.; Okumura, M.; Konno, T. Valence Interconversion of Octahedral Nickel(II/III/IV) Centers. *Angew. Chem., Int. Ed.* **2017**, *56*, 13762−13766. (f) Nebra, N. High-Valent NiIII and NiIV Species Relevant to C-C and C-Heteroatom Cross-Coupling Reactions: State of the Art. *Molecules* **2020**, *25*, 1141−1173.

(12) Robbins, J. L.; Edelstein, N.; Spencer, B.; Smart, J. C. Syntheses and electronic structures of decamethylmetallocenes. *J. Am. Chem. Soc.* **1982**, *104*, 1882−1893.

(13) (a) D'Accriscio, F.; Borja, P.; Saffon-Merceron, N.; Fustier-Boutignon, M.; Mézailles, N.; Nebra, N. C-H Bond Trifluoromethylation of Arenes Enabled by a Robust, High-Valent Nickel(IV) Complex. *Angew. Chem., Int. Ed.* **2017**, *56*, 12898−12902. (b) Watson, M. B.; Rath, N. P.; Mirica, L. M. Oxidative C-C Bond Formation Reactivity of Organometallic Ni(II), Ni(III), and Ni(IV) Complexes. *J. Am. Chem. Soc.* **2017**, *139*, 35−38. (c) Chong, E.; Kampf, J. W.; Ariafard, A.; Canty, A. J.; Sanford, M. S. Oxidatively Induced C-H Activation at High Valent Nickel. *J. Am. Chem. Soc.* **2017**, *139*, 6058−6061. (d) Meucci, E. A.; Nguyen, S. N.; Camasso, N. M.; Chong, E.; Ariafard, A.; Canty, A. J.; Sanford, M. S. Nickel(IV)-Catalyzed C-H Trifluoromethylation of (Hetero)arenes. *J. Am. Chem. Soc.* **2019**, *141*, 12872−12879.

(14) Herberich, G. E.; Wagner, T.; Marx, H. W. Borole derivatives XXI, 2,5-diphenyl-2,5,-dihydro-1H-boroles; strctures of tert-butyl-2,5,-diphenyl-2,5-dihydro-1H-borole and of bis(tmeda) lithium 2,5-diphenyl-2,5-dihydro-1H-boroledііde. *J. Organomet. Chem.* **1995**, *502*, 67−74.

(15) (a) Herberich, G. E.; Hostalek, M.; Laven, R.; Boese, R. Borole Dianions: Metalation of 1-(Dialkylamino)-2,5-Dihydro-1H-boroles and the Structure of $Li_2(C_4H_4BNEt_2)$·TMEDA. *Angew. Chem., Int. Ed. Engl.* **1990**, *29*, 317−318; *Angew. Chem.* **1990**, *102*, 330−331. (b) So, C. W.; Watanabe, D.; Wakamiya, A.; Yamaguchi, S. Synthesis and structural characterization of pentaarylboroles and their dianions. *Organometallics* **2008**, *27*, 3496−3501. (c) Lee, V. Y.; Sugasawa, H.; Gapurenko, O. A.; Minyaev, R. M.; Minkin, V. I.; Gornitzka, H.; Sekiguchi, A. From Borapyramidane to Borole Dianion. *J. Am. Chem. Soc.* **2018**, *140*, 6053−6056. (d) Herberich, G. E.; Buller, B.; Hessner, B.; Oschmann, W. Boron Derivatives, II. Pentaphenylborol: Synthesis, Reduction to Dianion and Complexes of Cobalt and Platinum. *J. Organomet. Chem.* **1980**, *195*, 253−259.

(16) (a) Fagan, P. J.; Burns, E. G.; Calabrese, J. C. Synthesis of Boroles and Their Use in Low-Temperature Diels-Alder Reactions with Unactivated Alkenes. *J. Am. Chem. Soc.* **1988**, *110*, 2979−2981. (b) Fagan, P. J.; Nugent, W. A.; Calabrese, J. C. Metallacycle Transfer from Zirconium to Main-Group Elements - a Versatile Synthesis of Heterocycles. *J. Am. Chem. Soc.* **1994**, *116*, 1880−1889. (c) Herberich, G. E.; Ohst, H. Derivatives of Borole, V. Synthesis of [1-(Diisopropylamino)Borole]Metal Complexes and the Diels-Alder Dimer of 1-(Diisopropylamino)Borole. *Chem. Ber.* **1985**, *118*, 4303−4313. (d) Su, X. J.; Baker, J. J.; Martin, C. D. Dimeric Boroles: Effective Sources of Monomeric Boroles for Heterocycle Synthesis. *Chem. Sci.* **2020**, *11*, 126−131.

(17) (a) Herberich, G. E.; Hessner, B.; Negele, M.; Howard, J. A. K. Borole Derivatives, X. Syntheses of (η^5-Borole)Metal Complexes Via Borole Ammonia Adducts. Complexes of the Chromium Group Metals and the Crystal and Molecular Structures of Tetracarbonyl [η^5-(1-Phenylborole)]Chromium and Its Molybdenum Analog. *J. Organomet. Chem.* **1987**, *336*, 29−43. (b) Herberich, G. E.; Negele, M. Derivatives of Borole, XII. Complexes of Nickel, Palladium and Platinum. (η^5-Borole)-(η^4-1,5-Cyclooctadiene)Metals and Bis(η^5-Borole)Metals. *J. Organomet. Chem.* **1988**, *350*, 81−89.

(18) (a) Herberich, G. E.; Hausmann, I.; Klaff, N. The 30-Electron Rule for Triple-Decker Complexes Vanadium, Niobium and Tantalum Complexes as Illustrative Examples. *Angew. Chem., Int. Ed. Engl.* **1989**, *28*, 319−320; *Angew. Chem.* **1989**, *101*, 328−329. (b) Herberich, G. E.; Boveleth, W.; Hessner, B.; Hostalek, M.; Koffer, D. P. J.; Negele, M. Borole Derivatives, IX. (η^5-Borole)Metal Complexes of Ruthenium, Osmium and Rhodium. *J. Organomet. Chem.* **1987**, *319*, 311−326. (c) Herberich, G. E.; Boveleth, W.; Hessner, B.; Koffer, D. P. J.; Negele, M.; Saive, R. Borole Derivatives, VI. Dehydrating Complexing of Borolenes with Carbonyl Metals. (Borole)Metal Complexes of Manganese, Iron and Cobalt. *J. Organomet. Chem.* **1986**, *308*, 153−166. (d) Herberich, G. E.; Hausmann, I.; Hessner, B.; Negele, M. Borole Derivatives, XIV. Dehydrating Complex-Formation of Borolenes with (Cyclopentadienyl)Nickel Complexes. *J. Organomet. Chem.* **1989**, *362*, 259−264.

(19) (a) Herberich, G. E.; Ohst, H. *Z. Naturforsch., B: J. Chem. Sci.* **1983**, *38*, 1388−1391. (b) Herberich, G. E.; Englert, U.; Hostalek, M.; Laven, R. *Chem. Ber.* **1991**, *124*, 17−23.

(20) (a) Herberich, G. E.; Negele, M.; Ohst, H. Derivatives of Borole, XVII. (η^5-[1-(Diisopropylamino)borole])metal Complexes: Syntheses, Protonation, Internal-Rotation. *Chem. Ber.* **1991**, *124*, 25−29. (b) Ruth, P. N.; Sindlinger, C. P. A Neutral "Aluminocene" Sandwich Complex: η^1- versus η^5-Coordination Modes of a Pentaarylborole with ECp* (E = Al, Ga; Cp*=C_5Me_5). *Angew. Chem., Int. Ed.* **2019**, *58*, 15051−15056; *Angew. Chem.* **2019**, *131*, 15193−15198.

(21) (a) Braunschweig, H.; Chiu, C. W.; Radacki, K.; Kupfer, T. Synthesis and Structure of a Carbene-Stabilized π-Boryl Anion. *Angew. Chem., Int. Ed.* **2010**, *49*, 2041−2044; *Angew. Chem.* **2010**, *122*, 2085−2088. (b) Braunschweig, H.; Dyakonov, V.; Jimenez-Halla, J. O. C.; Kraft, K.; Krummenacher, I.; Radacki, K.; Sperlich, A.; Wahler, J. An Isolable Radical Anion Based on the Borole Framework. *Angew. Chem., Int. Ed.* **2012**, *51*, 2977−2980; *Angew. Chem.* **2012**, *124*, 3031−3034.

(22) The chemical oxidation of **1** was attempted with $AgBF_4$, which gave an intractable mixture of products alongside copious amounts of nickel black.

(23) Attempts to generate **1** from reaction of 2 equiv of **L2** with $Ni(COD)_2$ were unsuccessful at 60, 80, or 110 °C overnight, with only **2** being observed as a product.

(24) (a) Reuter, D. C.; Thorne, L. R.; Gwinn, W. D. Infrared and Raman-Spectra and Normal Coordinate Analysis of Boranediamine. *J. Phys. Chem.* **1982**, *86*, 4737−4745. (b) Thorne, L. R.; Gwinn, W. D. Microwave spectra and molecular structure of $BH(NH_2)_2$. *J. Am. Chem. Soc.* **1982**, *104*, 3822−3827.

(25) Essex, L. A.; Taylor, J. W.; Harman, W. H. Nickel complexes of phosphine-appended benzannulated boron heterocycles. *Tetrahedron* **2019**, *75*, 2255−2260.

(26) Bond, A. M.; Colton, R.; Fiedler, D. A.; Field, L. D.; He, T.; Humphrey, P. A.; Lindall, C. M.; Marken, F.; Masters, A. F.; Schumann, H.; Sühring, K.; Tedesco, V. Coupled Redox Reactions, Linkage Isomerization, Hydride Formation, and Acid-Base Relationships in the Decaphenylferrocene System. *Organometallics* **1997**, *16*, 2787−2797.

(27) Frisch, G. W.; Trucks, M. J.; Schlegel, H. B.; Scuseria, G. E.; Robb, M. A.; Cheeseman, J. R.; Scalmani, G.; Barone, V.; Mennucci, B.; Petersson, G. A.; Nakatsuji, H.; Caricato, M.; Li, X.; Hratchian, H. P.; Izmaylov, A. F.; Bloino, J.; Zheng, G.; Sonnenberg, J. L.; Hada, M.; Ehara, M.; Toyota, K.; Fukuda, R.; Hasegawa, J.; Ishida, M.; Nakajima, T.; Honda, Y.; Kitao, O.; Nakai, H.; Vreven, T.; Montgomery, J. A., Jr.; Peralta, J. E.; Ogliaro, F.; Bearpark, M.; Heyd, J. J.; Brothers, E.; Kudin, K. N.; Staroverov, V. N.; Kobayashi, R.; Normand, J.; Raghavachari, K.; Rendell, A.; Burant, J. C.; Iyengar, S. S.; Tomasi, J.; Cossi, M.; Rega, N.; Millam, J. M.; Klene, M.; Knox, J. E.; Cross, J. B.; Bakken, V.; Adamo, C.; Jaramillo, J.; Gomperts, R.; Stratmann, R. E.; Yazyev, O.; Austin, A. J.; Cammi, R.; Pomelli, C.; Ochterski, J. W.; Martin, R. L.; Morokuma, K.; Zakrzewski, V. G.; Voth, G. A.; Salvador, P.; Dannenberg, J. J.; Dapprich, S.; Daniels, A. D.; Farkas, O.; Foresman, J. B.; Ortiz, J. V.; Cioslowski, J.; Fox, D. J. *Gaussian 09*, rev. D.01; Gaussian, Inc.: Wallingford, CT, 2013.

(28) Weigend, F.; Ahlrichs, R. Balanced basis sets of split valence, triple zeta valence and quadruple zeta valence quality for H to Rn:

https://doi.org/10.1021/acs.inorgchem.1c01845
Inorg. Chem. 2021, 60, 16160−16167

Design and assessment of accuracy. *Phys. Chem. Chem. Phys.* **2005**, *7*, 3297−3305.
(29) (a) Tang, H.; Guan, J.; Hall, M. B. Understanding the Radical Nature of an Oxidized Ruthenium Tris(thiolate) Complex and Its Role in the Chemistry. *J. Am. Chem. Soc.* **2015**, *137*, 15616−15619. (b) Tang, H.; Brothers, E. N.; Hall, M. B. The Distinctive Electronic Structures of Rhenium Tris(thiolate) Complexes, an Unexpected Contrast to the Valence Isoelectronic Ruthenium Tris(thiolate) Complexes. *Inorg. Chem.* **2017**, *56*, 583−593. (c) Tang, H.; Brothers, E. N.; Grapperhaus, C. A.; Hall, M. B. Electrocatalytic Hydrogen Evolution and Oxidation with Rhenium Tris(thiolate) Complexes: A Competition between Rhenium and Sulfur for Electrons and Protons. *ACS Catal.* **2020**, *10*, 3778−3789.

https://doi.org/10.1021/acs.inorgchem.1c01845
Inorg. Chem. 2021, 60, 16160−16167